ELSEVIER

Journal of Magnetism and Magnetic Materials 210 (2000) 341–348

Journal of magnetism and magnetic materials

www.elsevier.com/locate/jmmm

Magnetization reversal asymmetry in Fe/MgO(0 0 1) thin films

J.L. Costa-Krämer[a,*], J.L. Menéndez[a], A. Cebollada[a], F. Briones[a], D. García[b], A. Hernando[b]

[a]*Centro Nacional de Microelectrónica-IMM (CSIC), Isaac Newton 8 (PTM), Tres Cantos, Madrid 28760, Spain*
[b]*Instituto de Magnetismo Aplicado, P.O. Box 155, 28230 Las Rozas, Madrid, Spain*

Received 20 May 1999; received in revised form 13 September 1999

Abstract

We study the in-plane magnetization process in 200 Å Fe(0 0 1) thin films grown by sputtering at normal incidence. In spite of this growth geometry, a small uniaxial in plane magnetic anisotropy, whose origin is not totally understood, is found superimposed to the expected cubic biaxial one. This has a dramatic effect both on the reversal process and the domain structure. A combined longitudinal and transversal Kerr study shows the different switching processes (180° walls along the main easy axis versus 90° along the secondary easy axis) depending on the relative orientation of the magnetic field with respect to the Fe crystallographic axes. Remarkably, this two- and sometimes three-step switching process appears only when the field is applied along certain crystallographic directions. These findings are corroborated by domain observations.

PACS: 81.15.Cd; 75.70.Ak; 75.70.Kw

Keywords: Thin films; Fe; Domains; Anisotropy; Sputtering

1. Introduction

The study of growth and magnetic properties of epitaxial Fe thin films on insulator and semiconductor substrates has received much attention. Since the pioneering work of Prinz and Krebs [1], single-crystal Fe thin films have been grown on many different semiconductor substrates (for example, GaAs, ZnSe or Ge) [2] and insulators (such as MgO [3] or diamond [4]). Molecular beam epitaxy (MBE) and magnetron or RF sputtering are the standard growth techniques, while for the magnetic characterization, magneto-optic Kerr effect has proven to be a very accessible and versatile tool. All these films usually exhibit the expected in-plane four-fold magnetic anisotropy [5,6], due to the cubic structure of Fe, but often an additional uniaxial anisotropy is found superimposed [7]. This additional component of the anisotropy has been attributed to different origins, mainly caused by the geometry of the deposition system, through the lattice distortion induced by the angle of incidence of the deposited Fe atoms (therefore of magneto-elastic origin) [8–11], but also to the intrinsic anisotropy of the dangling bonds present in the growth on GaAs(0 0 1) [12]. On the other hand, the magnetization reversal process and magnetic

* Corresponding author. Tel.: 34-91-8060700; fax: 34-91-8060701.

E-mail address: kramer@imm.cnm.csic.es (J.L. Costa-Krämer)

0304-8853/00/$ - see front matter
PII: S0304-8853(99)00698-8

domain structure has also been studied in Fe/Ag(0 0 1) [13] or Fe/GaAs(0 0 1) [14,15] as-grown films, as well as on patterned Fe/GaAs(0 0 1) [16,17] and Fe/MgO(0 0 1) structures [18].

Here we present a study on the in-plane anisotropy and magnetization reversal process for Fe/MgO(0 0 1) thin films grown by triode sputtering at normal incidence. In spite of the non oblique growth configuration, a small uniaxial anisotropy is found superimposed to the expected four-fold cubic anisotropy. A combination of longitudinal and transversal Kerr investigation and magnetic domain observations allows us to discern the domain structure and magnetization reversal processes in these Fe single crystal films.

2. Experiment

The deposition of the films was performed in a triode-sputtering system with a base pressure in the low 10^{-9} mbar range. The substrate was first chemically cleaned in successive ultrasonic baths of tricloroethane, acetone, ethanol and distilled water. After loading into the growth chamber, it was outgassed overnight at 100°C and then annealed at 700°C for 1 h. Nominally, 200 Å of Fe were deposited at 50°C with an Ar pressure of 4×10^{-4} mbar, yielding growth rates of about 0.2 Å/s. A TiN capping layer nominally 15 Å thick was deposited on top by reactive sputtering to avoid oxidation of the Fe film. The structure was checked in situ by reflection high-energy electron diffraction (RHEED) and ex situ by X-ray diffraction (XRD). XRD experiments were performed using two different configurations: the Bragg–Brentano configuration with 1/4° slits plus a Cu secondary monochromator (Cu K_α radiation) for high angle scans; and, the high-resolution configuration with a Ge(2 2 0) four crystal monochromator (Cu K_{α_1} radiation) with 15 arcs beam divergence plus a 1/8° receiving slit for the low angle scans. The resulting reflectivity measurements were fitted using a code based on the recursion relation formalism of the Fresnel equations developed by Parratt [19,20]. Hysteresis loops with the magnetic field applied in the film plane were taken by the use of a combined transversal/longitudinal Kerr setup similar to the one described by Postava et al. [21]. We use either white light or a diode laser linearly polarized and focused on the sample, and a single photodiode in front of which a linear polarizer is either placed or removed in case of performing longitudinal or transversal Kerr measurements, respectively. The magnetic field was swept at a frequency of 2 Hz using Helmholtz coils. The photodiode data shown corresponds to a single-field cycle without any electronic filtering or averaging. The sample was mounted in a goniometer with 1° precision. The field direction was fixed. Magnetic domain imaging was performed using a home made low-field longitudinal Kerr setup including also a CCD camera, a PC video card and home-made software.

3. Growth and structure

The growth of crystalline Fe was checked in situ with RHEED and ex situ with XRD. Fig. 1(a) shows RHEED patterns for Fe film along [1 0 0] and [1 1 0] directions. Similar information is extracted by recording phi scans of both Fe(1 1 0) and MgO(2 2 0) asymmetric peaks (Fig. 1(b)). Besides, the expected 45° in-plane rotation of the Fe lattice with respect to the MgO one is confirmed. Fe lattice parameters are obtained from data taken by the combination of symmetric and asymmetric XRD scans yielding to values of (2.86 ± 0.01) and (3.03 ± 0.01) Å for the in-plane and perpendicular spacings, respectively. This means that Fe grows relaxed in the film plane but expanded in the growth direction by 5.8% when compared with the bulk lattice parameters. This result is in contrast with what has been previously observed by other groups, which either do not comment on any distortion on the Fe lattice or observe growth under a slight compression, yielding a perpendicular distortion of the Fe lattice parameter of about -0.5% to -0.6% either for sputtering [6] or MBE growth [9]. Nevertheless, Lairson et al. [22] have previously observed this vertical expansion in sputtered Fe/MgO(0 0 1), and correlated it with an islanded like growth for thicknesses less than 15 monolayers. Even though we are studying films 10 times thicker, one can assume a similar initial

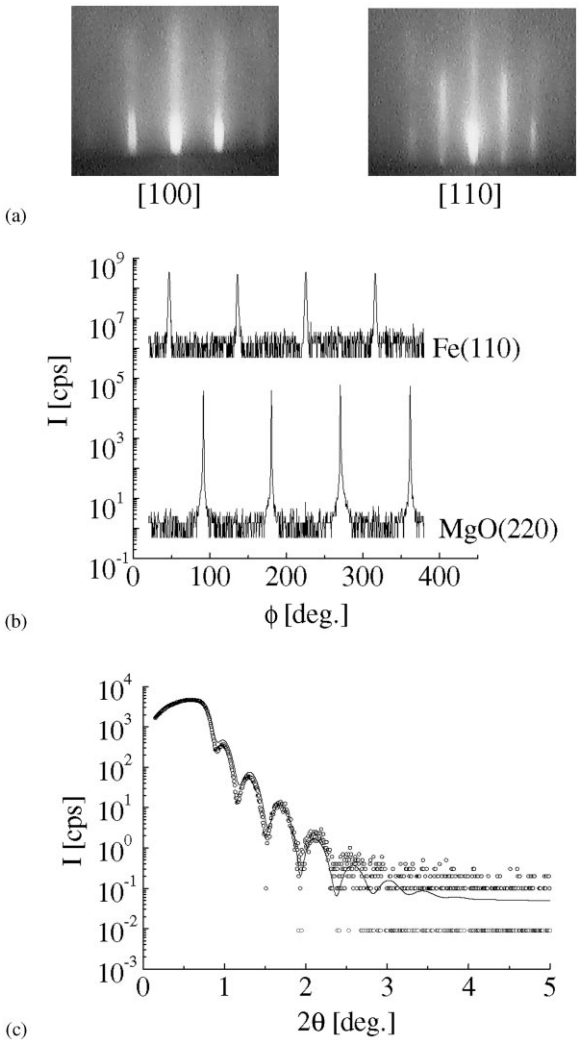

Fig. 1. Structural characterization: (a) RHEED pattern for the Fe/MgO(1 0 0) for two different azimuths; (b) XRD phi scan for MgO(2 2 0) and Fe(1 1 0) asymmetric diffraction peaks; (c) X-ray reflectometry curve (open circles) and best fit (solid line).

situation to the one described by Lairson at the first stages of growth, maintaining a big amount of residual strain as the film growth proceeds up to the total thickness. In our case, we have observed a systematic variation of this lattice expansion on changing growth conditions, work that will be presented in a subsequent paper. Other possible explanation for this lattice expansion involves the incorporation of interstitial Nitrogen in the Fe lattice during the TiN capping process [23]. An estimate of the crystalline coherence length along the growth direction yields an average value of 70 Å, applying Scherrer's equation to the width of the Fe(2 0 0) diffraction peak, the mosaic spread of the same peak being 2.15°. Accurate values of film thickness and interface roughness are obtained through fittings to the X-ray reflectometry data (Fig. 1(c)), yielding to values of 198 Å Fe, 19 Å TiN and typical interface roughness of 10 Å (rms) between substrate and Fe, and 8 Å (rms) between Fe and TiN and between TiN and air.

4. Magnetic characterization

As mentioned in the introduction, our 200 Å single-crystal BCC Fe thin film displays a magnetic behaviour consistent with the cubic crystalline structure. This is observed with in-plane magneto-optic hysteresis loops and with domain observations at the surface, both types of measurements correlating well.

The in-plane magnetic remanence as a function of the applied field angle with respect to the in-plane Fe crystallographic directions is shown in Fig. 2, together with the corresponding hysteresis loops. Note that the reduced remanence (M_r/M_s) is 1 when the field is applied along Fe [1 0 0] directions and $(M_r/M_s) \approx 0.7 \approx (\cos 45^\circ)$ when the field is applied along the Fe [1 1 0] direction. This is expected for preferred domain orientations pointing along the easy [1 0 0] direction. When the field is applied along these easy directions the reversal takes place by the nucleation and subsequent propagation of domain walls. When the field is applied along the hard [1 1 0] directions, this irreversible switch in the easy direction is followed by a continuous reversible rotation of the magnetization from the [1 0 0] to the [1 1 0] direction. The obtained value for the anisotropy constant K_1, assuming the bulk saturation magnetization value, is of the expected order of magnitude for Fe. Thus, the domain distribution at remanence at 45° with respect to the applied field direction produces the observed M_r/M_s value. An important feature, not easily observable from the polar plot, but evident from the observation of the different hysteresis

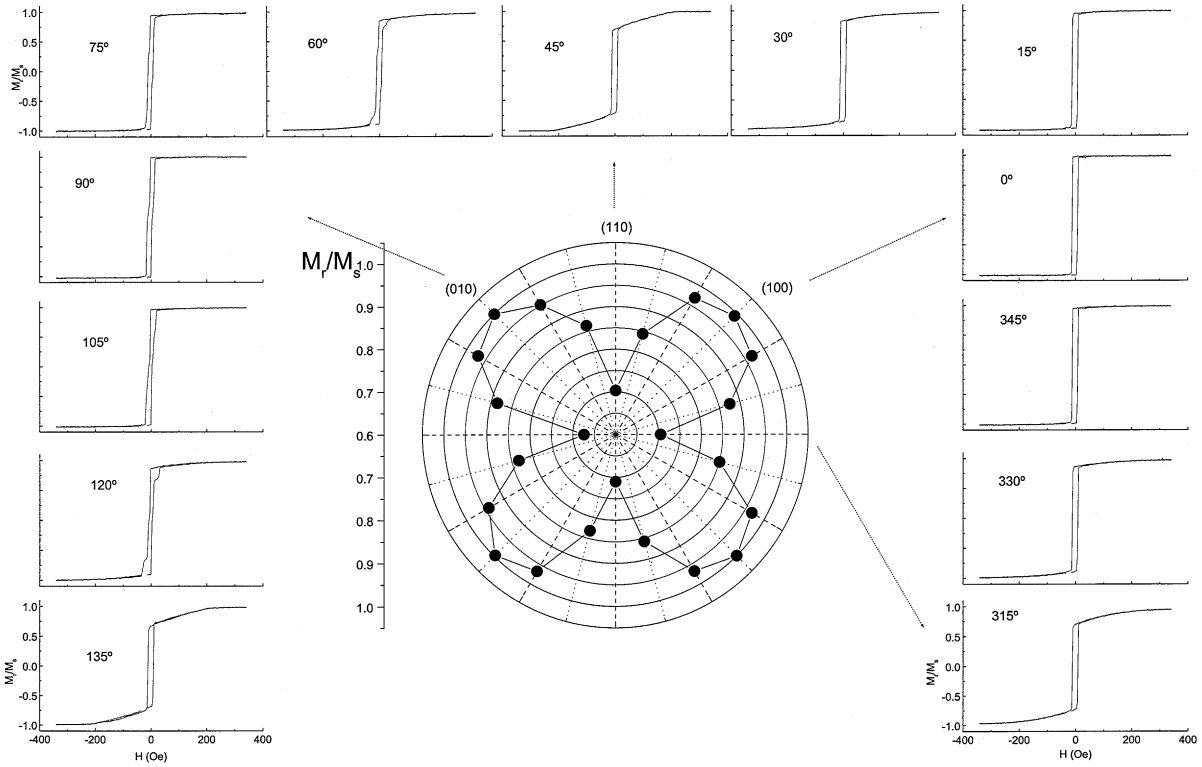

Fig. 2. Longitudinal hysteresis loops with the magnetic field applied along different in plane directions; Center: polar plot showing M_r/M_s versus the applied field angle.

loops, is that applying the magnetic field along equivalent crystallographic directions does not produce equivalent hysteresis loops. This is obvious when comparing loops obtained for symmetric orientations, such as 60° and 30°, 75° and 15°, 90° and 0°, and so on.

In order to investigate this asymmetry further a set of low-field Kerr magneto-optic loops were recorded. In addition to the Kerr reflectivity changes, proportional to the magnetization component parallel to the applied field, the Kerr rotation was also measured to obtain the magnetization component perpendicular to the applied field. This procedure obtains both projections of the average magnetization as a function of the applied field and allows us to discern the operative magnetization processes. As mentioned above, the low-field behaviour is investigated in detail due to the presence of reversal anomalies that we attribute to the presence of a small uniaxial anisotropy of unclear origin. This extra anisotropy is not evident in the polar plot, which allows us to give an upper bound for the anisotropy value of the order of the error bar which is about 3% of the bulk Fe magnetocrystalline anisotropy value. Its direction would be perpendicular to the quadrants where the two- and sometimes three-stage switching takes place, i.e., parallel to the [1 0 0] direction. Some possible origins of this uniaxial anisotropy have been mentioned in the introduction and, in addition, residual magnetic fields present in the chamber could be also responsible. However, test experiments designed to check this possibility produced a negative result. The substrate texture is, in our opinion, the most possible source for the extra anisotropy in this system, such as steps, as previously demonstrated for Fe on stepped W(0 0 1) [24]. The low-field loops are shown in Fig. 3, where the relative orientation of the

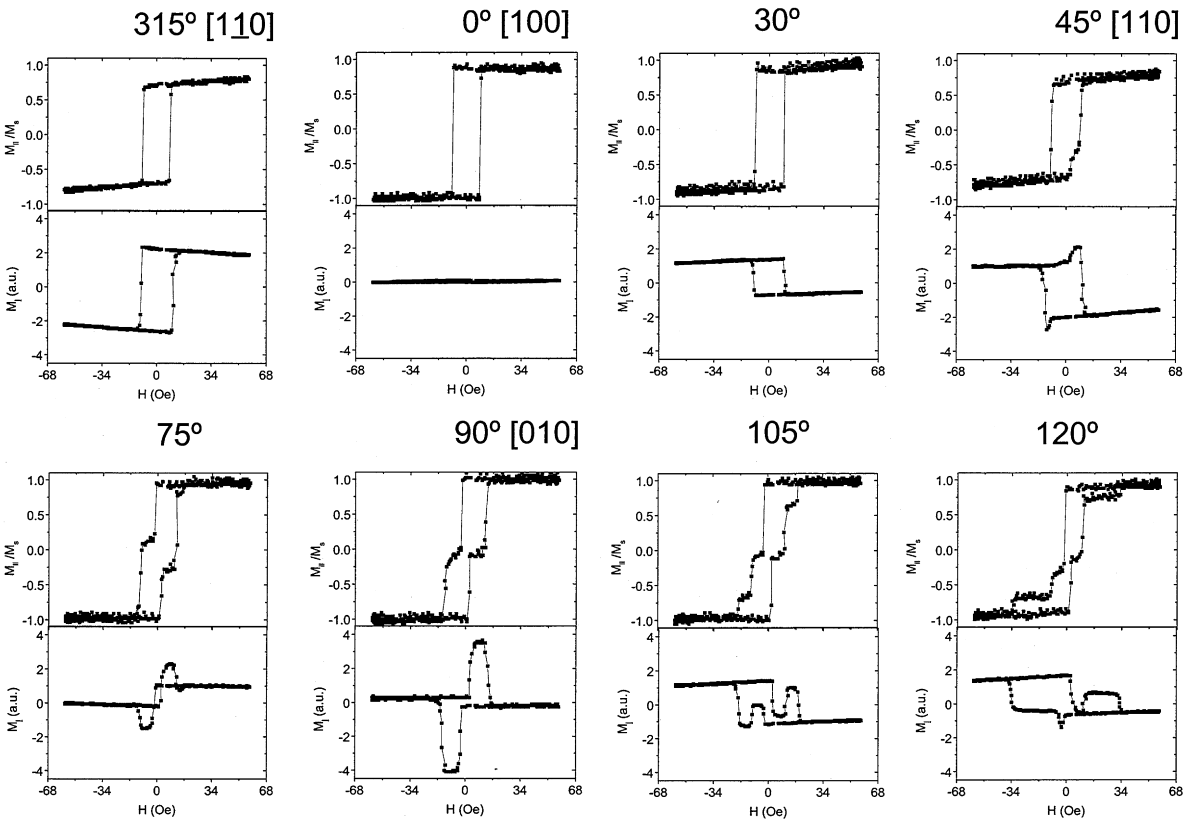

Fig. 3. Hysteresis loops showing the longitudinal and transverse magnetization components for different azimuths.

magnetic field with the crystallographic axes is varied continuously. The first loop corresponds to a situation where the magnetic field is applied along the hard [1 1̄ 0] direction. Both longitudinal and perpendicular components of the magnetization switch simultaneously, pointing to 180°-domain wall movement as the operative magnetization process. This switching occurs at 45° with respect to the field direction. When the magnetic field is applied along the [1 0 0] direction, the longitudinal component switches again in one clear Barkhausen jump, but this time no transverse signal is detected during the field cycle. This evidences as well 180° wall propagation, but with the magnetization now aligned parallel to the field. On increasing the angle further, at 30° with respect to the easy axis, we recover the detection of both longitudinal and transversal components, the last one of opposite sign to the one detected along the hard axis [1 1̄ 0] as expected. On applying the magnetic field along the [1 1 0] hard direction the magnetization no longer switches in a single jump, an anomalous behaviour which is more apparent in the transverse component. Note the difference with the [1 1̄ 0] loop that is, in principle, an equivalent direction. This behaviour becomes more pronounced and reaches a maximum when the field is applied along the [0 1 0] easy direction. Now, the longitudinal magnetization switches in two clear Barkhausen jumps. These are separated by a plateau which constitutes an intermediate state that is accompanied by a high transversal signal observed at the same field values. This implies that at the plateau the magnetization lies mostly along the

perpendicular [1 0 0] easy direction, pointing out to 90° domain wall propagation as the operative magnetization process between saturation and plateau. This is in contrast with the loop obtained along the [1 0 0] direction, where the magnetization switching in a single 180° Barkhausen jump within our experimental resolution. This two-stage process is more clear-cut in the transverse magnetization. For intermediate directions, such as the labelled 75°, 105° and 120°, the magnetization switching does not occur in a single step, but in two, and sometimes three distinct processes that can be explained by intermediate states where the magnetization lies perpendicular to the [0 1 0] direction as explained above. This behaviour is described in detail also in Ref. [14]. Note that this multiple step switching is only observed in the quadrant between 45° and 135°. This behaviour clearly separates from the one expected for a simple biaxial in-plane anisotropy, and can be explained by the existence of a superimposed uniaxial anisotropy, which makes behave unequivalently, from the magnetic point of view, directions that are equivalent from the crystallographic point of view.

The magnetic behaviour reported so far would be consistent with a single-domain picture with coherent magnetization rotations and reversals. In order to investigate the domain structure associated to the different magnetization reversal processes, we performed MOKE domain observations at selected loop positions. Figs. 4 and 5 show hysteresis loops together with the corresponding magnetic domains, for the situations where the magnetic field is applied along the two unequivalent easy axis. The hysteresis loop corresponding to the main easy axis (Fig. 4(a)) has a perfect square shape with single and abrupt magnetization switching at about 7 Oe. Zones I and II correspond to the situations just before and after switching of the magnetization direction. The associated domain distribution is shown in Fig. 4(b) and (c), for an applied magnetic field of -6.5 (zone I) and -7.5 Oe (zone II), respectively. The remanent state (I) exhibits a single-domain distribution. Domain distribution for the state (II) shows almost complete reversal of magnetization, except for a narrow line that crosses almost completely the sample surface and some areas close to the edges of

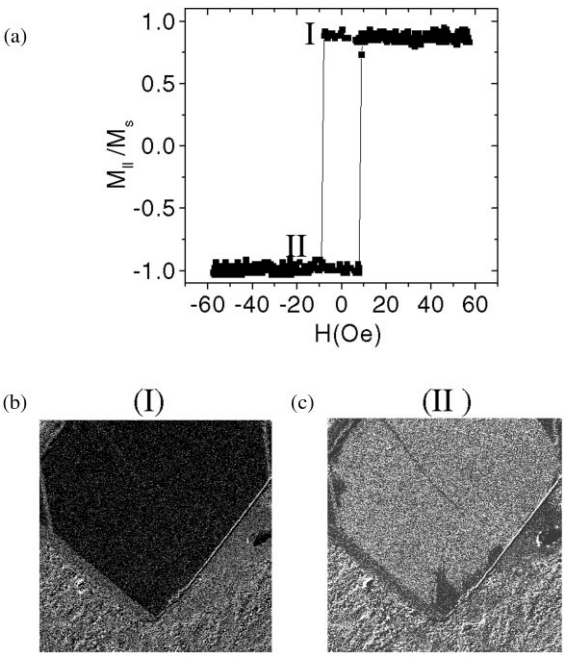

Fig. 4. (a) Kerr hysteresis loop taken with the magnetic field applied in-plane along the main easy axis; (b) and (c) Kerr domain images taken in the above configuration for magnetic fields of -6.5 and -7.5 Oe, respectively.

the sample; in both cases it is due to macroscopic morphological defects on the sample surface. These results corroborate the 180° domain wall picture of the magnetization reversal along this direction.

On the other hand, the hysteresis loop corresponding to the secondary easy axis (Fig. 5(a)) shows the already mentioned plateaus at low fields. Detailed domain observations, indicate that the very first stages of magnetization reversal are characterized by large, up to 1 mm domains magnetized along the main easy axis (white domains in the figure) that nucleate, propagate via 90°, walls and pin at surface structural defects. Further increase of magnetic field produces the appearance reversed black domains that grow from the pinning sites. These experimental facts have allowed us to assign the magnetization orientations in Fig. 5(b)–(e) which show the domain distribution corresponding to the selected zones in the hysteresis loop (III–IV). III is indicative of a remanent state, IV and V correspond to intermediate states and VI to the reversed magnetization state. For the remanent state

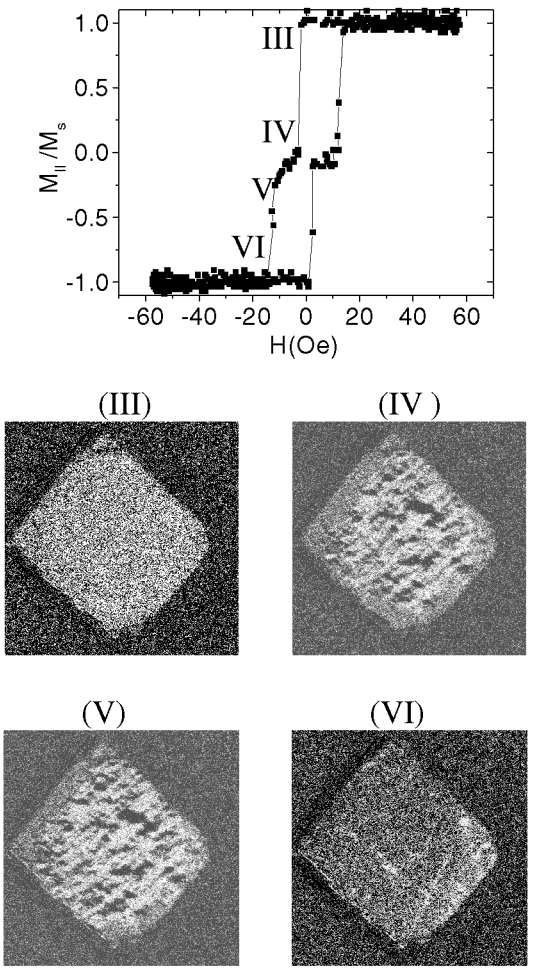

Fig. 5. (a) Kerr hysteresis loop taken with the magnetic field applied in-plane along the secondary easy axis. (b), (c), (d) and (d) Kerr domain images taken in the above configuration for magnetic fields of 0, -4, -6 and -16 Oe, respectively. See text for the domain direction assignment.

(III), the domain distribution is again uniform characteristic of a single domain. Zones IV and V basically exhibit three different regions: grey areas, corresponding to domains whose magnetizations have not reversed yet, black areas corresponding to reversed magnetization zones, and light areas corresponding to domains with magnetizations perpendicular to the secondary axis, i.e., along the main one and perpendicular to the applied magnetic field. Further application of magnetic field leads to zone VI, with a uniform single-domain magnetization distribution, corresponding to saturation, again except of some macroscopic morphological defects.

5. Conclusions

The magnetization reversal process has been studied for Fe thin films grown by triode sputtering at normal incidence. The remanent state is well described by a cubic biaxial anisotropy, with the magnetization along [1 0 0] directions independently of the applied field direction. However, the low-field magnetization dynamics reflects the existence of a small uniaxial anisotropy superimposed over the biaxial crystalline anisotropy, leading to the inequivalency of crystalline easy axes. A single-jump transition driven by 180° domain wall movement is observed when the magnetic field is applied along the main easy axis. A two-stage process driven by 90° domain wall movement is observed when the field is applied along the secondary easy axis. In addition, there is an angular range where two- and sometimes three-stage processes driven by 90° domain wall movement are observed. In all these cases, the reversal is via an intermediate state in which at least three-domain orientations coexist. This demonstrates again the inequivalency of the easy axes and the dramatic effect it has on both the magnetization reversal and the domain structure. The most possible cause, in our opinion, for this additional uniaxial anisotropy is the surface texture present in the MgO substrate.

Acknowledgements

This work was carried out under financial support of the Spanish Commission of Science and Technology. One of us, J. L. Menéndez, would like to acknowledge Comunidad de Madrid's Consejería de Educación y Cultura for financial support.

References

[1] G.A. Prinz, J.J. Krebs, Appl. Phys. Lett. 39 (1981) 397.

[2] G.A. Prinz, Magnetic metal films on semiconductor substrates, in: B. Heinrich, J.A.C. Bland (Eds.), Ultrathin Magnetic Structures, Springer, Berlin, 1994, pp. 1–42 and references therein.
[3] P. Etienne, J. Massies, S. Lequien, R. Cabanel, F. Petroff, J. Crystal Growth 111 (1991) 1003.
[4] D.P. Pappas, J.W. Glesener, V.G. Harris, Y. Idzerda, J.J. Krebs, G.A. Prinz, Appl. Phys. Lett. 64 (1994) 28.
[5] Yu.V. Goryunov, N.N. Garif'yanov, G.G. Khaliullin, I.A. Garifullin, Phys. Rev. B 52 (1995) 13450.
[6] B. Li, J.R. Fermin, A. Azevedo, F.M. de Aguiar, S.M. Rezende, Appl. Phys. Lett. 72 (1998) 2760.
[7] R.P. Cowburn, S.J. Gray, J. Ferre, J.A.C. Bland, J. Miltat, J. Appl. Phys. 78 (1995) 7210.
[8] J.R. Childress, R. Kergoat, O. Durand, J.M. George, P. Galtier, J. Miltat, A. Schuhl, J. Magn. Magn. Mater. 130 (1994) 13.
[9] O. Durand, J.R. Childress, P. Galtier, R. Bisaro, A. Schuhl, J. Magn. Magn. Mater. 145 (1995) 111.
[10] R.P. Coburn, S.J. Gray, J. Ferré, J.A.C. Bland, J. Miltat, J. Appl. Phys. 78 (1995) 7210.
[11] K. Postava, H. Jaffres, A. Schuhl, F. Nguyen Van Dau, M. Goiran, A.R. Fert, J. Magn. Magn. Mater. 172 (1997) 199.
[12] M. Zölfl, M. Brockmann, M. Köhler, S. Kreuzer, T. Schweinböck, S. Miethaner, F. Bensch, G. Bayreuther, J. Magn. Magn. Mater. 175 (1997) 16.
[13] R.P. Coburn, J. Ferré, S.J. Gray, J.A.C. Bland, Phys. Rev. B 58 (1998) 11507.
[14] E. Gu, J.A.C. Bland, C. Daboo, M. Gester, L.M. Brown, R. Poessl, J.N. Chapman, Phys. Rev. B 51 (1995) 3596.
[15] C. Daboo, R.J. Hicken, E. Gu, M. Gester, S.J. Gray, D.E.P. Eley, E. Ahmad, J.A.C. Bland, R. Ploessl, J.N. Chapman, Phys. Rev. B 51 (1995) 15964.
[16] U. Ebels, A.O. Adeyeye, M. Gester, C. Daboo, R.P. Cowburn, J.A.C. Bland, J. Appl. Phys. 81 (1997) 4724.
[17] U. Ebels, A.O. Adeyeye, M. Gester, R.P. Cowburn, C. Daboo, J.A.C. Bland, Phys. Rev. B 56 (1997) 5443.
[18] H. Jaffrès, L. Ressier, J.P. Peyrade, A.R. Fert, P. Gogol, A. Thiaville, A. Schul, F. Nguyen Van Dau, J. Appl. Phys. 84 (1998) 4375.
[19] T.A. Rabedeau, M.F.Toney, unpublished.
[20] L.G. Parrat, Phys. Rev. 95 (1954) 359.
[21] K. Postava, J.F. Bobo, M.D. Ortega, B. Raquet, H. Haffres, E. Snoek, M. Goiran, A.R. Fert, J.P. Redoules, J. Pistora, J.C. Ousset, J. Magn. Magn. Mater. 163 (1996) 8.
[22] B.M. Lairson, A.P. Payne, S. Brennan, N.M. Rensing, B.J. Daniels, J. Appl. Phys. 78 (1995) 4449.
[23] K. Uchiyama, R.C. O'Handley, IEEE Trans. Magn. 35 (1999) 2024.
[24] H.J. Choi, Z.Q. Qiu, J. Pearson, J.S. Jiang, D. Li, S.D. Bader, Phys. Rev. B 57 (1998) R12713.